Analytical Analysis of a Squeeze-Film Dominated MEMS Fluid Ejector

E. P. Furlani and J. A. Lebens

Integrated Materials and Microstructures Laboratory, Eastman Kodak Company,
Rochester, New York 14650-2011, edward.furlani@kodak.com, john.lebens@kodak.com

ABSTRACT

We present an analytical model for predicting the behavior of a squeeze-film dominated MEMS fluid ejector. The ejector consists of a piston that is driven toward a nozzle plate with a relatively thin layer of fluid sandwiched between the two (Fig. 1). We derive an expression for the pressure distribution generated by the moving piston, and develop a lumped-element model for predicting the piston motion. We use the model to study device performance.

Keywords: Microfluidics, MEMS, squeeze film, drop ejection, analytical analysis, drop-on-demand.

1 INTRODUCTION

MEMS fluid ejection systems are being used in a wide range of applications including micro-dose drug delivery, ink-jet printing, and various biomedical and chemical micro-dispensers. An electrostatically actuated MEMS ejection system has been fabricated at Sandia National Laboratories using the SUMMiT process [1]. In this device, the piston is supported in its rest position by polysilicon springs, and drop ejection occurs when the piston is electrostatically accelerated toward the nozzle plate. The Sandia ejector has an operating frequency of 10 kHz and produces 2-4 picoliter drops moving at 10 m/s. To date, this device has been simulated as an axisymmetric finite element model using the GOMA program. The dominant pressure mechanism is due to the squeeze-film effect. In this paper we derive an expression for the pressure distribution generated by the moving piston, and develop an analytical model for predicting the device performance. Our model yields results in agreement with the prior GOMA analysis. We use it to study device performance as a function of variations in the reservoir gap g, with the input power fixed. Our analysis shows that the drop volume and velocity degrade as the gap decreases, but the volumetric efficiency increases. This is due to the movement of the fluid stagnation point away from the orifice as the gap decreases. Our model enables rapid parametric analysis of device performance, and is of considerable use in the development of novel MEMS fluid ejectors.

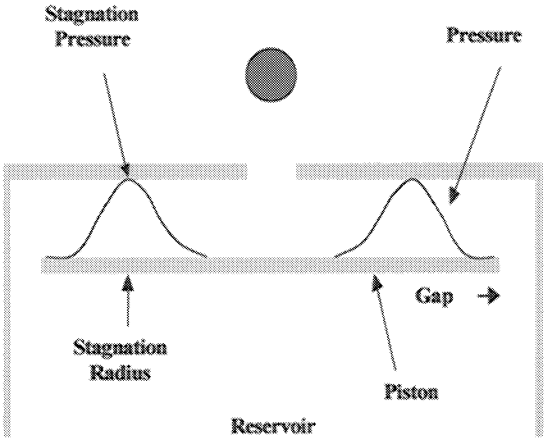

Figure 1: Axisymmetric fluid ejector.

2 THEORY

We model the fluid ejector using a lumped-element analysis. The motion of the piston is obtained from the equation for the force balance on the piston

$$\left(m_p + m_{eff}(t)\right)\frac{dv_p}{dt} = F_a(t) - kx_p(t) - 2\pi\int_0^{r_p} p(r, v_p, t)\, r\, dr + \sum F_f \qquad (1)$$

where m_p, $x_p(t)$, and $v_p(t)$ are the mass, position, and velocity of the piston, $m_{eff}(t)$ is the effective mass of the fluid that it accelerates, $F_a(t)$ is the applied force, k is a spring constant of the polysilicon support members, $p(r, v_p, t)$ is the squeeze-film pressure distribution acting on the piston, and $\sum F_f$ represents other forces due to the fluid motion. In the following sections we obtain expressions for the dominant terms in Eq. (1).

2.1 Squeeze-Film Analysis

In this section we derive an expression for the pressure distribution developed by the moving piston. We apply Reynolds lubrication theory to the axisymmetric geometry shown in Fig. 1. The pressure satisfies the following differential equation

$$\frac{1}{r}\frac{\partial}{\partial r}\left(r\frac{\partial p(r,t)}{\partial r}\right)=-\frac{12\mu}{h^3}v_p(t) \qquad (r_0 \le r \le r_p) \tag{2}$$

where r_o and r_p are the radius of the orifice and the piston respectively, and h is the distance from the piston to the nozzle plate. The general solution to this equation is of the form

$$p(r,t)=-\frac{3\mu v_p(t)}{h^3}r^2 + c_1\ln(r) + c_2, \tag{3}$$

where c_1 and c_2 are constants determined form the boundary conditions [2]. The pressure distribution (3) peaks at a value p_s at the stagnation radius $r_s(t)$,

$$r_s(t)=\sqrt{\frac{h^3 c_1}{6\mu v_p(t)}}, \tag{4}$$

as shown in Fig. 1.

The boundary conditions for this problem are

$$\begin{aligned} p(r,t) &= p_B(t) \qquad (r=r_o) \\ p(r,t) &= p_R(t) \qquad (r=r_p) \end{aligned} \tag{5}$$

where $p_B(t)$ and $p_R(t)$ are the pressures beneath the orifice $(r \le r_o)$, and at the edge of the piston, respectively. We determine expressions for $p_B(t)$ and $p_R(t)$ by considering the volume flow rates through the orifice and into the reservoir, respectively.

The volume flow rate through the orifice due to the piston motion is

$$Q_o(t)=\pi r_s^{\,2}(t)v_p(t). \tag{6}$$

The fluid is considered to be incompressible, and therefore the velocity of the fluid exiting the orifice is given by

$$v_o(t)=\frac{r_s^{\,2}(t)v_p(t)}{r_o^{\,2}}. \tag{7}$$

We use Eq. (7) to estimate the Bernoulli pressure $p_B(t)$,

$$p_B(t)=\frac{1}{2}\rho\frac{r_s^{\,4}(t)v_p^{\,2}(t)}{r_o^{\,4}} \tag{8}$$

Similarly, the flow rate into the reservoir is given by

$$Q_R(t)=\pi\left(r_p^{\,2}-r_s^{\,2}\right)v_p(t) \tag{9}$$

This flow rate can be is related to the pressure $p_R(t)$ and the piston velocity $v_p(t)$,

$$Q_R(t)=\alpha p_R(t)+g\pi r_p v_p(t), \tag{10}$$

where $\alpha=\dfrac{(2\pi r_p)g^3}{12\mu d_p}$, μ is the viscosity of the fluid, and d_p is the thickness of the piston. The first and second terms in Eq. (10) account for Poiseuille and Couette flows through the gap, respectively. From Eqs. (9) and (10) we obtain

$$p_R(t)=\frac{1}{\alpha}\left[\pi\left(r_p^{\,2}-r_s^{\,2}\right)-g\pi r_p\right]v_p(t) \tag{11}$$

We solve Eqs. (3)-(5), (8) and (11) simultaneously and obtain formulas for $p_B(t)$, c_1, and c_2. Specifically, we find that

$$p_B(t)=\left(\frac{-b^2+\sqrt{b^2-4c(t)}}{2}\right)^2 \tag{12}$$

where

$$b=-\frac{6\mu r_p^{\,2}}{h^3}\sqrt{\frac{2}{\rho}}\left[\ln(r_o/r_p)-\frac{\pi h^3}{6\alpha\mu}\right], \tag{13}$$

and

$$c(t)=-\left[\frac{3\mu}{h^3}\left(r_p^{\,2}-r_o^{\,2}\right)+\frac{\pi r_p^{\,2}}{\alpha}\right]v_p(t), \tag{14}$$

and that

$$c_1=\frac{6\mu r_p^{\,2}}{h^3}\sqrt{\frac{2p_B(t)}{\rho}}, \tag{15}$$

and

$$c_2=p_B(t)+\frac{3\mu r_0^{\,2}}{h^3}v_p(t)-c_1\ln(r_o). \tag{16}$$

The stagnation radius r_s (t) is obtained from Eq. (4).

2.2 Effective Mass

We take into account inertial effects by estimating the mass of fluid accelerated by the piston as it moves. As above, we assume that the fluid within the stagnation radius flows towards the orifice, while the fluid beyond this point flows through the gap into the reservoir. We consider the flow towards the orifice first. We assume that the mass of fluid within the stagnation radius accelerates at the same

rate as the piston itself. Thus, the effective mass of this fluid is

$$m_s(t) = \rho\left(h_0 - x_p(t)\right)\pi r_s^{\,2}(t), \tag{17}$$

where h_0 is the initial distance between the nozzle plate and the piston in its rest position, and $x_p(t)$ is the distance of the piston from its rest position, respectively.

Next, we consider the flow through the nozzle. Since the fluid is incompressible, the volume flow rate through the orifice is given by Eq. (6), and the average acceleration of this flow is

$$a_o(t) = \frac{r_s^{\,2}}{r_o^{\,2}} a_p(t). \tag{18}$$

The effective mass associated with this flow is

$$m_o(t) = \rho l_0 \pi r_s^{\,2}, \tag{19}$$

where l_o is the thickness of the nozzle plate.

We now consider the flow into the reservoir. Let $\bar{v}(r,t)$ denote the average velocity of the fluid at a distance $(r_s < r < r_p)$ beyond the stagnation radius. When the piston moves we find that that,

$$\frac{d\bar{v}(r,t)}{dt} = \frac{\left(r^2 - r_s^{\,2}\right)}{2r\left(h_0 - x_p(t)\right)}\left[a_p(t) + \frac{v_p^{\,2}(t)}{\left(h_0 - x_p(t)\right)}\right] \tag{20}$$

This gives rise to a force of the form,

$$F(t) = \rho\pi\left[\frac{r_p^{\,3} + 2r_s^{\,3}}{3} - r_s^{\,2} r_p\right] a_p(t) + \rho\pi\left[\frac{r_p^{\,3} + 2r_s^{\,3}}{3} - r_s^{\,2} r_p\right]\frac{v_p^{\,2}(t)}{\left(h_0 - x_p(t)\right)} \tag{21}$$

The first term can be treated as an effective mass, which we call m_R,

$$m_R = \rho\pi\left[\frac{r_p^{\,3} + 2r_s^{\,3}}{3} - r_s^{\,2} r_p\right]. \tag{22}$$

The second term in Eq. (21) is a force that needs to be included in the $\sum F_f$ term in Eq. (1).

Finally, we consider the acceleration of fluid through the gap. From the conservation of mass we know that

$$a_g(t) = \frac{\left(r_p^{\,2} - r_s^{\,2}(t)\right)}{2r_p g} a_p(t). \tag{23}$$

Therefore, the effective mass of this fluid is

$$m_g = \rho\pi l_p\left(r_p^{\,2} - r_s^{\,2}(t)\right). \tag{24}$$

From our analysis we find that the total effective mass of the fluid is

$$m_{eff}(t) = \rho\pi\left[\frac{r_p^{\,3} + 2r_s^{\,3}(t)}{3} - r_s^{\,2} r_p\right] + \rho\pi l_0 r_s^{\,2}(t) + \rho\pi\left(h_0 - x_p(t)\right) r_s^{\,2}(t) + \rho\pi l_p\left(r_p^{\,2} - r_s^{\,2}(t)\right) \tag{25}$$

2.3 Equation of Motion

The equation of motion Eq. (1) contains an expression $\sum F_f$ that accounts for additional forces due to fluid flow. Two such forces arise from the flow across orifice/air and gap/reservoir interfaces. These additional forces have the form,

$$F_o(t) = \rho\pi r_o^{\,2} v_o^{\,2}(t), \tag{26}$$

and

$$F_g(t) = \rho 2\pi r_p g\, v_g^{\,2}(t), \tag{27}$$

where $v_g(t)$ is the average velocity across the gap/reservoir interface. We collect all the relevant terms and obtain the following equation of motion for the piston

$$\left(m_p + m_{eff}(t)\right)\frac{dv_p}{dt} = F_a(t) - kx_p(t) - \pi r_o^{\,2} p_B(v_p,t) - 2\pi\int_{r_o}^{r_p} p(r,v_p,t)\, r\, dr - \rho\frac{\pi^2\left(r_p^{\,2} - r_s^{\,2}\right)^2}{\left(2\pi r_p g\right)} v_p^{\,2}(t) - \rho\pi\frac{r_s^{\,4}}{r_o^{\,2}} v_p^{\,2}(t) - \rho\pi\left[\frac{r_p^{\,3} + 2r_s^{\,3}}{3} - r_s^{\,2} r_p\right]\frac{v_p^{\,2}(t)}{\left(h_0 - x_p(t)\right)} \tag{28}$$

To perform device simulation, we integrate this nonlinear ODE using a fourth-order Runge-Kutta method. We present some sample calculations in the next section.

3 RESULTS

We use Eq. (28) to study the behavior of the drop ejector. To estimate the drop velocity, we track the momentum P_d and mass M_d of the fluid exiting the orifice,

$$P_d = \int_0^{\tau} \rho Q_o(t) v_o(t) dt, \tag{29}$$

and

$$M_d = \int_0^{\tau} \rho Q_o(t) dt, \tag{30}$$

where τ is the duration of the applied voltage. The drop velocity is given by

$$V_d = P_d / M_d. \tag{31}$$

This analysis does not take into account the complex free-surface phenomenon of necking at the orifice, and therefore will over estimate the drop velocity. We impose an additional constraint that the fluid will flow trough the orifice only when the Bernoulli pressure exceeds the Laplace pressure $2\sigma / r_0$ (σ is the surface tension),

$$Q_o(t) = \begin{cases} 0 & p_B < 2\sigma / r_o \\ \pi r_o^2 v_o(t) & p_B \geq 2\sigma / r_o \end{cases} \tag{32}$$

We apply our model to an ejector with the following parameters: $r_o = 10\mu m$, $r_p = 60\mu m$, and k = 25 N/m. The reservoir gap is taken to be infinity, and the fluid is water. We apply a constant electric field of E = 25 V/micron for a period of $\tau = 4.4\mu s$. Therefore, the applied force is $F_a(t) = \varepsilon\pi\left(r_p^2 - r_o^2\right)E^2/2$ where $\varepsilon = 70\varepsilon_0$. We compute the drop velocity and volume for two different initial heights $h_0 = 4.5$ and $5.5\mu m$. We obtain drop volumes of 2.8 and 3.36 picoliters, respectively with velocities of 10 and 10.47 m/s. This represents a 120% increase in drop volume for the larger h_0, which is in agreement with Gooray et al., who report a 126% increase for a similar geometry [1].

Next, we study the device performance as a function of the reservoir gap g. We set $r_o = 10\mu m$, $r_p = 100\mu m$, and k = 100 N/m. We fix the applied voltage at 60 V for $\tau = 2.5\mu s$. Our analysis shows that drop volume and velocity degrade modestly as the gap approaches 3 um, and then more rapidly below that value (Figs. 2 and 3). The peak stagnation pressure and piston displacement follow a similar trend. However, the volumetric efficiency increases dramatically as the gap decreases indicating that a higher fraction of the fluid displaced by the piston is ejected though the orifice. The reason for this is that the stagnation radius increases with decreasing gap. These results are also in agreement with the work of Gooray et al. [1].

The analysis of this section takes only a few minutes on a personal computer. Therefore, our analytical model is useful for understanding the ejector physics, and for performing rapid parametric analysis.

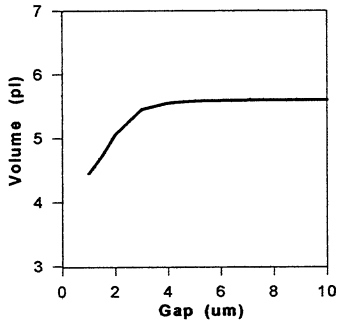

Figure 2: Drop volume vs reservoir gap.

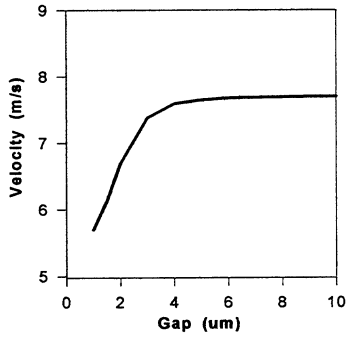

Figure 3: Drop velocity vs reservoir gap.

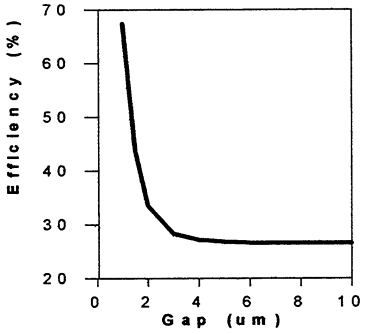

Figure 4: Volumetric efficiency vs reservoir gap.

REFERENCES

[1] A. Gooray, G. Roller, P. Galambos, K. Zavadll, R. Givler, F. Peter, and J. Crowley, "Design of a MEMS Ejector for Printing Applications," Journal of Imaging Science and Technology, Vol. 46, No. 5, 415-432, 2002.

[2] A. H. Burr and J. B. Cheatham, *Mechanical Analysis and Design*, Second Edition, Prentice Hall, New Jersey, 1995.